Efficient System Reliability Analysis of Slope Stability in Spatially Variable Soils Using Monte Carlo Simulation

Shui-Hua Jiang[1]; Dian-Qing Li, M.ASCE[2]; Zi-Jun Cao[3]; Chuang-Bing Zhou[4]; and Kok-Kwang Phoon, F.ASCE[5]

Abstract: Monte Carlo simulation (MCS) provides a conceptually simple and robust method to evaluate the system reliability of slope stability, particularly in spatially variable soils. However, it suffers from a lack of efficiency at small probability levels, which are of great interest in geotechnical design practice. To address this problem, this paper develops a MCS-based approach for efficient evaluation of the system failure probability $P_{f,s}$ of slope stability in spatially variable soils. The proposed approach allows explicit modeling of the inherent spatial variability of soil properties in a system reliability analysis of slope stability. It facilitates the slope system reliability analysis using representative slip surfaces (i.e., dominating slope failure modes) and multiple stochastic response surfaces. Based on the stochastic response surfaces, the values of $P_{f,s}$ are efficiently calculated using MCS with negligible computational effort. For illustration, the proposed MCS-based system reliability analysis is applied to two slope examples. Results show that the proposed approach estimates $P_{f,s}$ properly considering the spatial variability of soils and improves the computational efficiency significantly at small probability levels. With the aid of the improved computational efficiency offered by the approach, a series of sensitivity studies are carried out to explore the effects of spatial variability in both the horizontal and vertical directions and the cross-correlation between uncertain soil parameters. It is found that both the spatial variability and cross-correlation affect $P_{f,s}$ significantly. The proposed approach allows more insights into such effects from a system analysis point of view. **DOI: 10.1061/(ASCE)GT.1943-5606.0001227.**

Author keywords: Slope stability; System reliability; Monte Carlo simulation (MCS); Representative slip surface; Stochastic response surface; Spatial variability.

Introduction

Uncertainties are unavoidable in slope engineering, such as the inherent spatial variability of geotechnical properties (Vanmarcke 1977a, b) and uncertainties associated with deterministic calculation models for estimating the safety margin of slope stability. Among these uncertainties, the inherent spatial variability of geotechnical properties has been considered to be one of the major sources of uncertainties in geotechnical properties (Christian et al. 1994; Phoon and Kulhawy 1999; Ching and Phoon 2013; Lloret-Cabot et al. 2014). It significantly affects the slope stability (Griffiths and Fenton 2004; Cho 2007, 2010; Huang et al. 2010; Wang et al. 2011; Ji et al. 2012; Jiang et al. 2014a; Tabarroki et al. 2013; Li et al. 2014). One primary effect of the inherent spatial variability on slope stability is that the critical slip surface with minimum factor of safety ($FS_{\min}$) varies spatially when the spatial variability is considered (Wang et al. 2011). Identification of the critical slip surface among a large number of potential slip surfaces is an elementary step in slope stability analysis. From a system analysis point of view, the slope can be viewed as a series system (Chowdhury and Xu 1995; Li et al. 2009, 2011b), in which each potential slip surface is a component and the critical slip surface is the weakest one. System failure occurs as the slope slides along the critical slip surface. Under a probabilistic framework, slope reliability analysis is then defined as a system reliability analysis problem, in which the overall failure probability (or system failure probability, $P_{f,s}$) of a slope considering numerous potential slip surfaces is of interest and it is greater than the failure probability of any individual potential slip surface because of system effects (Cornell 1967; Ditlevsen 1979). System reliability analysis of slope stability has been gaining increasing interest during the past decade (Oka and Wu 1990; Chowdhury and Xu 1995; Ching et al. 2009; Low et al. 2011; Zhang et al. 2011, 2013; Ji and Low 2012). These previous studies have demonstrated that there might exist multiple dominating failure modes (or slip surfaces) in slope stability analysis problems, and these failure modes are considered rationally during the system reliability analysis of slope stability. However, most of the previous studies focused on various slope failure modes (i.e., slip surfaces) caused by stratification (i.e., layered soils), and the inherent spatial variability of soil properties in each soil layer is rarely considered.

[1]Graduate Student, State Key Laboratory of Water Resources and Hydropower Engineering Science, Key Laboratory of Rock Mechanics in Hydraulic Structural Engineering (Ministry of Education), Wuhan Univ., Wuhan 430072, P.R. China.

[2]Professor, State Key Laboratory of Water Resources and Hydropower Engineering Science, Key Laboratory of Rock Mechanics in Hydraulic Structural Engineering (Ministry of Education), Wuhan Univ., Wuhan 430072, P.R. China (corresponding author). E-mail: dianqing@whu.edu.cn

[3]Associate Professor, State Key Laboratory of Water Resources and Hydropower Engineering Science, Key Laboratory of Rock Mechanics in Hydraulic Structural Engineering (Ministry of Education), Wuhan Univ., Wuhan 430072, P.R. China.

[4]Professor, State Key Laboratory of Water Resources and Hydropower Engineering Science, Key Laboratory of Rock Mechanics in Hydraulic Structural Engineering (Ministry of Education), Wuhan Univ., Wuhan 430072, P.R. China.

[5]Professor, Dept. of Civil and Environmental Engineering, National Univ. of Singapore, Singapore 117576.

Note. This manuscript was submitted on January 14, 2014; approved on September 24, 2014; published online on October 14, 2014. Discussion period open until March 14, 2015; separate discussions must be submitted for individual papers. This paper is part of the ***Journal of Geotechnical and Geoenvironmental Engineering***, © ASCE, ISSN 1090-0241/04014096 (13)/$25.00.

To explicitly incorporate the inherent spatial variability into a system reliability analysis of slope stability, Griffiths and Fenton (2004) and Huang et al. (2010) applied a random FEM and Monte Carlo simulation (MCS) to evaluate the system reliability of slope stability in spatially variable soils, and Cho (2010) combined random field theory and MCS to assess $P_{f,s}$ based on limit-equilibrium methods [e.g., simplified Bishop method (Duncan and Wright 2005)]. Although MCS is a conceptually simple and robust method for probabilistic analysis (Wang et al. 2011; Wang 2013), it suffers from a lack of efficiency at small probability levels, which are of particular interest in slope engineering practice. This drawback of MCS becomes even more profound for slope reliability analysis in spatially variable soils, because the critical slip surface varies spatially and needs to be located for each random sample generated during the MCS. To improve the efficiency of MCS-based slope reliability analysis, Wang et al. (2011) used an advanced MCS method called subset simulation to calculate $P_{f,s}$, and Li et al. (2013) developed a MCS-based risk deaggregation approach for the system reliability analysis of slope stability. In their studies, the inherent spatial variability along the depth is modeled explicitly using a one-dimensional (1D) random field. Despite these efforts, how to efficiently evaluate the system reliability of slope stability remains a difficult problem, particularly when multidimensional [e.g., two-dimensional (2D) or three-dimensional] spatial variability is considered.

This paper develops an efficient system reliability analysis approach based on MCS and limit-equilibrium methods to evaluate the $P_{f,s}$ of slope stability in spatially variable soils. The proposed approach allows explicit modeling of the inherent spatial variability in the system reliability analysis of slope stability and improves the computational efficiency of slope system reliability analysis using representative slip surfaces (RSSs) and multiple stochastic response surfaces. The paper starts with probabilistic modeling of the inherent spatial variability of soil properties in both the horizontal and vertical directions and cross-correlation between soil properties, followed by the system reliability analysis of slope stability and construction of stochastic response surfaces. Then, implementation procedures for the proposed approach are described. Finally, the proposed approach is illustrated through two slope examples with one single soil layer. A series of sensitivity studies are also performed using the two examples to explore the effects of the inherent spatial variability and cross-correlation on the system reliability of slope stability.

Probabilistic Modeling of Spatially Variable Soils

Random field theory (Vanmarcke 1977a, b) is applied in this study to explicitly model the inherent spatial variability of relevant soil properties, such as the undrained shear strength c_u for cohesive soils and the cohesion c and friction angle ϕ for c-ϕ soils. Let H denote the uncertain soil property of interest, and its inherent spatial variability in the horizontal and vertical directions can be modeled by a 2D lognormal stationary random field $\underline{H}(x,y)$ with a mean μ_H and SD σ_H, where x is the horizontal coordinate on a bounded domain Ω, and it varies from 0 to L_x, i.e., $0 \le x \le L_x$; y is the vertical coordinate on a bounded domain Ω, and it ranges from 0 to L_y, i.e., $0 \le y \le L_y$; and L_x and L_y are the lengths of Ω in the horizontal and vertical directions, respectively, and they are greater than zero by definition. Because the statistics of statistically homogeneous random fields only depend on relative distance, rather than absolute locations, Ω can be defined in several alternative manners [e.g., $\Omega = \{(x,y): -L_x/2 \le x \le L_x/2; -L_y/2 \le y \le L_y/2\}$] provided that the dimensions (i.e., L_x and L_y) in the horizontal and vertical directions remain the same. In this study, Ω is defined as $\{(x,y): 0 \le x \le L_x; 0 \le y \le L_y\}$ only for mathematical convenience. In addition, it shall be noted that a lognormal random field is applied in this study, because the lognormal random variable is a continuous variable and strictly nonnegative, which complies with the physical meaning of most geotechnical parameters (e.g., c_u, c, and ϕ). The lognormal random field is frequently used to model the inherent spatial variability of geotechnical parameters and has been shown to perform well in the geotechnical literature (Griffiths et al. 2002; Griffiths and Fenton 2004; Cho 2010; Tabarroki et al. 2013).

In the context of random field theory, the spatial correlation between the variations of the considered soil property at different locations is described by a spatial autocorrelation structure. In this paper, the autocorrelation structure is taken as a squared exponential autocorrelation function, and the autocorrelation coefficient between the logarithm [i.e., $\ln(H)$] of H at different locations [e.g., (x_1, y_1) and (x_2, y_2)] is calculated as (Fenton and Griffiths 2008)

$$\rho_{\ln}[(x_1,y_1),(x_2,y_2)] = \exp\left\{-\left[\left(\frac{|x_1-x_2|}{\theta_{\ln,h}}\right)^2 + \left(\frac{|y_1-y_2|}{\theta_{\ln,v}}\right)^2\right]\right\} \tag{1}$$

where $\theta_{\ln,h}$ and $\theta_{\ln,v}$ = horizontal and vertical autocorrelation distances, respectively. With Eq. (1), the random field $\underline{H}(x,y)$ can be efficiently simulated using series expansion methods, such as Karhunen-Loève (K-L) expansion (Ghanem and Spanos 2003; Phoon et al. 2002; Cho 2010; Jiang et al. 2014a). For practical implementation and concise representation, $\underline{H}(x,y)$ is truncated up to the order of M. Then, under K-L expansion, the lognormal random field $\underline{H}(x,y)$ is expressed as

$$\underline{H}(x,y) = \underline{H}(x,y;\theta) = \exp\left[\mu_{N,H} + \sum_{j=1}^{M} \sigma_{N,H}\chi_j(\theta)\right], \quad (x,y) \in \Omega \tag{2}$$

where $\mu_{N,H} = \ln(\mu_H) - \sigma_{N,H}^2/2$ and $\sigma_{N,H} = \sqrt{\ln(1+\sigma_H^2/\mu_H^2)}$ = mean and SD of $\ln(H)$, respectively; $\chi_j(\theta) = \sqrt{\lambda_j} f_j(x,y)\xi_j(\theta)$, $j = 1, 2, \ldots, M$ = set of spatially correlated standard normal random variables (i.e., a standard normal random field); θ = coordinate in the decomposed outcome space; $\xi_j(\theta)$, $j = 1, 2, \ldots, M$ = set of independent standard normal random variables; and λ_j and $f_j(x,y)$, $j = 1, 2, \ldots, M$ = eigenvalues and eigenfunctions of the autocorrelation function [Eq. (1)], respectively. Specifically, λ_j and $f_j(x,y)$ can be obtained by solving the homogeneous Fredholm integral equation of the second kind (Phoon et al. 2002; Cho 2010). The determination of M in Eq. (2) relies on the desired accuracy and autocorrelation function [Eq. (1)] adopted in random fields. In this study, M is determined to ensure that $\varepsilon = \sum_{i=1}^{M}\lambda_i / \sum_{i=1}^{\infty}\lambda_i$ is greater than 95%, in which the λ_i are sorted in a descending order, so that the total variance of $\underline{H}(x,y)$ within the considered domain Ω is basically preserved (Marzouk and Najm 2009; Laloy et al. 2013; Jiang et al. 2014a). Interested readers are referred to Marzouk and Najm (2009), Laloy et al. (2013), and Jiang et al. (2014a) for more details and explanations on choosing the value of M.

Note that only the autocorrelation of a single soil property H (e.g., c_u, c, or ϕ) is explicitly modeled in Eq. (2). In practice, two or even more soil properties might be considered as uncertain parameters in each soil layer. Consider, for example, c and ϕ in a c-ϕ soil layer. Their standard normal random fields $\underline{\chi}_c(\theta) = \{\chi_{c,j}(\theta), j = 1,2,\ldots,M\}$ and $\underline{\chi}_\phi(\theta) = \{\chi_{\phi,j}(\theta), j = 1,2,\ldots,M\}$ that account for the autocorrelation of each parameter can be generated first. Then, the correlation between c and ϕ, namely, cross-correlation, is taken into account by (Fenton and Griffiths 2003; Jiang et al. 2014a)

$$\underline{c}(x,y) = \underline{c}(x,y;\theta) \approx \exp\left[\mu_{N,c} + \sum_{j=1}^{M} \sigma_{N,c}\chi_{c,j}(\theta)\right], \quad (x,y) \in \Omega \tag{3}$$

$$\underline{\phi}(x,y) = \underline{\phi}(x,y;\theta) \approx \exp\left\{\mu_{N,\phi} + \sum_{j=1}^{M} \sigma_{N,\phi}\left[\chi_{c,j}(\theta)\rho_{c\text{-}\phi,N} + \chi_{\phi,j}(\theta)\sqrt{1-\rho_{c\text{-}\phi,N}^2}\right]\right\}, \quad (x,y) \in \Omega \tag{4}$$

where $\mu_{N,c} = \ln(\mu_c) - \sigma_{N,c}^2/2$ and $\sigma_{N,c} = \sqrt{\ln(1+\sigma_c^2/\mu_c^2)}$ = mean and SD of $\ln(c)$, respectively; $\mu_{N,\phi} = \ln(\mu_\phi) - \sigma_{N,\phi}^2/2$ and $\sigma_{N,\phi} = \sqrt{\ln(1+\sigma_\phi^2/\mu_\phi^2)}$ = mean and SD of $\ln(\phi)$, respectively; μ_c and σ_c = mean and SD of c, respectively; μ_ϕ and σ_ϕ = mean and SD of ϕ, respectively; and $\rho_{c\text{-}\phi,N}$ = cross-correlation coefficient between $\ln(c)$ and $\ln(\phi)$, which can be calculated from the cross-correlation coefficient (i.e., $\rho_{c\text{-}\phi}$) between c and ϕ (Fenton and Griffiths 2008). Note that Eqs. (3) and (4) account for both the autocorrelation of c and ϕ and the cross-correlation between them. They allow for the efficient simulation of the cross-correlated lognormal random fields of c and ϕ in the MCS-based system reliability analysis of slope stability, which is discussed in the "MCS-Based System Reliability Analysis of Slope Stability" section.

MCS-Based System Reliability Analysis of Slope Stability

Slope failure occurs when the slope slides along any slip surface. In theory, there may exist an infinite number of potential slip surfaces. Evaluating the overall failure probability (i.e., system failure probability, $P_{f,s}$) along all the potential slip surfaces is a mathematically formidable task (El-Ramly et al. 2002). Therefore, $P_{f,s}$ is frequently calculated using a large, but finite, number of potential slip surfaces. Let $S_1, S_2, \ldots, S_{N_s}$ denote N_s potential slip surfaces that are considered in the limit-equilibrium analysis of slope stability. Then, the slope can be considered as a series system that consists of N_s components (i.e., $S_1, S_2, \ldots, S_{N_s}$). The system failure occurs when any component (i.e., $S_1, S_2, \ldots, S_{N_s}$) fails. The system failure probability $P_{f,s}$ can be calculated using MCS (Li et al. 2013)

$$P_{f,s} = \frac{1}{N_t}\sum_{k=1}^{N_t} I(FS_{\min} < 1) \tag{5}$$

where N_t = total number of samples generated during MCS; $FS_{\min}$ = minimum FS value among FS values of the N_s potential slip surfaces for a given set of random samples of uncertain parameters $\underline{X}$ (i.e., c_u, c, and ϕ) involved in slope stability analysis; and $I\{\cdot\}$ = indicator function. For a given random sample, $I(FS_{\min} < 1)$ is taken as the value of 1 when $FS_{\min} < 1$ occurs. Otherwise, it is equal to zero.

Note that the slip surface with $FS_{\min}$ (i.e., critical slip surface) needs to be located among N_s potential slip surfaces for each random sample generated during MCS, and its corresponding $FS_{\min}$ is calculated using a deterministic slope stability analysis method, such as limit-equilibrium methods [e.g., simplified Bishop method (Duncan and Wright 2005)]. To ensure that the critical slip surface is properly located, a large number of potential slip surfaces are usually considered in deterministic slope stability analysis, i.e., N_s is large. The value of N_s is frequently on the order of magnitude of 10^3-10^4 (Zhang et al. 2011; Li et al. 2013). Performing MCS for slope reliability analysis based on such a large number of potential slip surfaces requires extensive computational efforts, particularly in spatially variable soils, because the critical slip surface varies spatially when spatial variability is considered (Wang et al. 2011).

Several previous studies (Zhang et al. 2011, 2013; Ji and Low 2012; Li et al. 2013; Cho 2013) have suggested using some RSSs, which dominate the slope failure, as a surrogate for the large number of potential slip surfaces to evaluate $FS_{\min}$ for each random sample. The number N_r of RSSs is generally much less than that (i.e., N_s) of potential slip surfaces (Zhang et al. 2011; Li et al. 2013). Therefore, the critical slip surface can be identified among RSSs with relative ease, and $FS_{\min}$ can be calculated more efficiently during MCS. This subsequently leads to efficient evaluation of the system reliability of slope stability. In this study, the RSSs are used in the MCS-based system reliability analysis of slope stability, and a stochastic response surface is constructed for each RSS to calculate the FS of the RSS during MCS, by which the computational efficiency of the MCS-based system reliability analysis of slope stability is further improved, as discussed in the "Multiple Stochastic Response Surfaces for RSSs" section.

Multiple Stochastic Response Surfaces for RSSs

To facilitate the calculation of $FS_{\min}$ in the MCS-based system reliability analysis of the slope, this study applies Hermite polynomial chaos expansion to construct a stochastic response surface for each RSS. Under the Hermite polynomial chaos expansion, FS for a given RSS is calculated as (Huang et al. 2009; Li et al. 2011a; Al-Bittar and Soubra 2013; Jiang et al. 2014b)

$$FS_{j_r}(\underline{\boldsymbol{\xi}}) = a_0\Gamma_0 + \sum_{i_1=1}^{N} a_{i_1}\Gamma_1(\xi_{i_1}) + \sum_{i_1=1}^{N}\sum_{i_2=1}^{i_1} a_{i_1,i_2}\Gamma_2(\xi_{i_1},\xi_{i_2}) + \sum_{i_1=1}^{N}\sum_{i_2=1}^{i_1}\sum_{i_3=1}^{i_2} a_{i_1,i_2,i_3}\Gamma_3(\xi_{i_1},\xi_{i_2},\xi_{i_3}) + \cdots \tag{6}$$

where $j_r = 1, 2, \ldots, N_r$; $N = M \times N_F$ = number of random variables in standard normal space; N_F = number of random fields involved in slope reliability analysis; M = order of the series used in the K-L expansion of random fields [Eqs. (2)–(4)]; $a_0, a_{i_1}, a_{i_1,i_2}, a_{i_1,i_2,i_3}, \ldots$ = unknown coefficients; $\Gamma_{j_p}(\cdot), j_p = 1, 2, 3, \ldots$ = Hermite polynomials with j_p degrees of freedom (Ghanem and Spanos 2003; Huang et al. 2009; Li et al. 2011a); and $\underline{\boldsymbol{\xi}} = (\xi_1, \xi_2, \ldots, \xi_N)$ = set of independent standard normal random variables corresponding to those used to discretize the random fields by K-L expansion [Eq. (2)]. From a physical point of view, the stochastic response surface given by Eq. (6) is a surrogate for the slope stability analysis model that involves uncertain geotechnical parameters, and provides an explicit and approximate functional relationship to predict the FS of slope stability considering the uncertainties (Huang et al. 2009; Li et al. 2011a).

For the n_{HPCE}th-order Hermite polynomial chaos expansion, there are a total of $(N + n_{\text{HPCE}})!/(N! \times n_{\text{HPCE}}!)$ unknown coefficients (i.e., $a_0, a_{i_1}, a_{i_1,i_2}, a_{i_1,i_2,i_3}, \ldots$) in Eq. (6), which need to be determined for the construction of the stochastic response surfaces. Determination of these unknown coefficients requires N_p realizations of the random variables (or random fields) involved in slope reliability analysis and their corresponding N_p FS values for each RSS estimated from the conventional deterministic slope stability analysis. The N_p realizations of random fields can be generated by Latin hypercube sampling (LHS) using Eq. (2) or Eqs. (3) and (4) (Choi et al. 2006). Based on the N_p random samples and their corresponding FS values for a given RSS, N_p linear equations are

obtained using Eq. (6). Then, the unknown coefficients are determined by solving these N_p linear equations. After that, the stochastic response surface for the RSS concerned is obtained. The accuracy of the stochastic response surface relies on the order (i.e., n_{HPCE}) of the Hermite polynomial chaos expansion, the number (i.e., N) of random variables involved in the reliability analysis, and the accuracy of the estimated coefficients (i.e., $a_0, a_{i_1}, a_{i_1,i_2}, a_{i_1,i_2,i_3}, \ldots$). The accuracy of the estimated coefficients in this study also depends on the number (i.e., N_p) of realizations of random fields used to determine the unknown coefficients, random field element mesh, and deterministic slope stability analysis method used to estimate FS of slope stability. The effects of these three factors on the results obtained from this study are further discussed in the "Discussion" section.

The procedure described previously is repeated for the N_r RSSs to obtain their respective stochastic responses surfaces. During MCS, the N_r stochastic responses surfaces are, collectively, used as a surrogate for the conventional deterministic slope analysis to explicitly and efficiently evaluate $FS_{\min}$ for each random sample. In this way, the computational cost used for each random sample is substantially reduced and so are the total computational costs of MCS.

Note that, for the construction of the N_r stochastic response surfaces, there needs to be a selection of N_r RSSs among all the potential slip surfaces and a determination of the N_p FS values for each RSS. These are achieved simultaneously in this study through a simple and practical procedure. The procedure starts by generating N_p realizations of the random fields involved in the slope reliability analysis. For each of the N_p realizations of random fields, a conventional deterministic analysis (e.g., simplified Bishop method) is performed to calculate the FS values for all the potential slip surfaces and to locate the critical slip surface with $FS_{\min}$. This is repeated N_p times, leading to N_r critical slip surfaces. These N_r critical slip surfaces are used as RSSs in this study, where N_r is less than or equal to N_p, because different realizations of random fields might result in the same critical slip surface. In addition, the repeated calculations for the N_p realizations of random fields simultaneously lead to N_p FS values for each RSS. These N_p FS values for the RSS are subsequently used to construct its corresponding stochastic response surface using Eq. (6). By these means, the selection of RSSs and the determination of the stochastic response surface for each RSS are achieved simultaneously, and no additional computational efforts are required to identify the RSSs for the system reliability analysis of slope stability.

Implementation Procedure

Fig. 1 shows a flowchart for the implementation of the proposed MCS-based system reliability analysis approach schematically. In general, the implementation procedure involves five steps. The details of each step and its associated equations are summarized as follows.

1. Determine input information for the system reliability analysis of slope stability, including but not limited to the slope geometry and statistics (e.g., mean, SD, marginal distribution, cross-correlation coefficient, autocorrelation function, and autocorrelation distance) of the soil properties.
2. Generate N_p realizations of random fields by LHS according to prescribed statistical information using Eq. (2) for independent random fields or Eqs. (3) and (4) for cross-correlated random fields.
3. Perform a limit-equilibrium analysis (e.g., simplified Bishop method) of slope stability with the N_p realizations of random fields generated in Step 2 to determine N_r RSSs and calculate N_p FS values for each RSS.

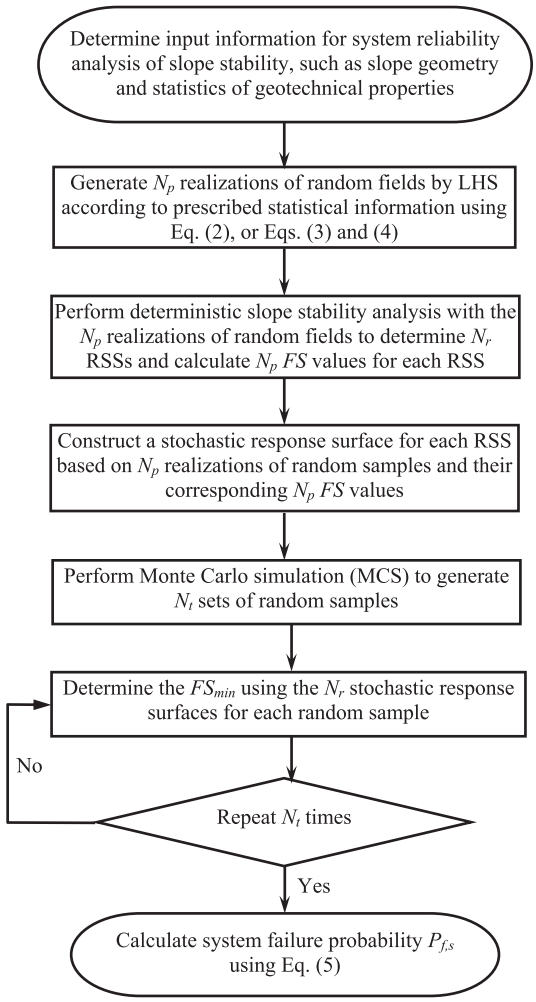

Fig. 1. Flowchart for implementation

4. Construct N_r stochastic response surfaces [Eq. (6)] for the N_r RSSs based on the N_p random samples and their corresponding N_p FS values.
5. Perform the MCS to generate N_t random samples in the independent standard normal space to estimate the system failure probability $P_{f,s}$ using Eq. (5), where $FS_{\min}$ for each random sample is determined using the N_r stochastic response surfaces obtained in Step 4.

The proposed MCS-based system reliability analysis approach for slope stability and its previously described implementation procedures can be programmed as a software package with the aid of commercial software packages for deterministic slope stability analysis, such as *SLOPE/W 2007*. The software package can be divided into three modules: the deterministic slope stability analysis module (e.g., *SLOPE/W*), the stochastic response surface module, and the MCS module. By these means, the deterministic slope stability analysis is deliberately decoupled from the reliability analysis (including the construction of stochastic response surfaces and MCS for uncertainty propagation), so that the reliability analysis of slope stability can proceed as an extension of the deterministic slope stability analysis in a nonintrusive manner. This effectively removes the hurdle of a reliability computational algorithm and allows geotechnical practitioners to focus on the deterministic slope stability analysis that they are familiar with, which will facilitate wider implementation of the proposed approach.

In addition, it is worthwhile to emphasize that the N_r stochastic response surfaces used in the MCS are explicit functions between uncertain input parameters and FS, and hence, the computational effort required for calculating $FS_{\min}$ during MCS is minimal. After the N_r stochastic response surfaces are obtained, $P_{f,s}$ is calculated efficiently using MCS. The main computational effort used for the proposed approach is that spent on the construction of N_r stochastic response surfaces, which is generally much less than the computational effort needed for direct implementation of a MCS with conventional deterministic slope stability analysis in spatially variable soils, particularly at small probability levels. This is further illustrated through a cohesive slope example and a c-ϕ slope example in the "Illustrative Example I: Cohesive Slope" and "Illustrative Example II: c-ϕ Slope" sections, respectively.

Illustrative Example I: Cohesive Slope

This section applies the proposed MCS-based system reliability analysis approach to analyze a saturated cohesive slope example under an undrained condition, which has been analyzed by Cho (2010) to demonstrate the probabilistic analysis of slope stability in spatially variable soils. As shown in Fig. 2, the cohesive slope has a height of 5 m and a slope angle of 26.6°. The cohesive soil layer extends to 10 m below the top of the slope and has a total unit weight of 20 kN/m^3. In the cohesive soil layer, the short-term strength is characterized using the undrained shear strength c_u, and the inherent spatial variability of c_u is explicitly modeled using a 2D lognormal stationary random field $\underline{c}_u$ with a mean μ_{c_u} of 23 kPa, a coefficient of variation (COV) COV_{c_u} of 0.3, a horizontal autocorrelation distance $\theta_{\ln,h}$ of 20 m, and a vertical autocorrelation distance $\theta_{\ln,v}$ of 2.0 m. These statistics are the same as those adopted by Cho (2010). As shown in Fig. 2, the random field $\underline{c}_u$ is discretized into 910 elements with a side length of 0.5 m for its realization, and its random samples are then generated using Eq. (2) at the centroid of each element, in which M is taken as 15 to ensure that the ε-value is larger than 95% in this example. As a reference, the nominal value of $FS_{\min}$ that corresponds to the case of all the c_u being equal to its mean value (i.e., 23 kPa) is calculated using the simplified Bishop method (Duncan and Wright 2005), and it is equal to 1.356, which is identical to the value reported by Cho (2010). In addition, the critical slip surface in the nominal case is also located and is shown in Fig. 2. It is referred to as the critical deterministic slip surface (CDSS) in this example.

For the identification of RSSs and the construction of their respective stochastic response surfaces, 1,000 (i.e., $N_p = 1{,}000$) realizations of $\underline{c}_u$ are simulated by LHS using Eq. (2), and their corresponding critical slip surfaces are determined using the simplified Bishop method and are taken as RSSs in this example, resulting in a total of 71 RSSs, as shown in Fig. 3. Note that the CDSS identified in the nominal case (see the dashed line in Fig. 3) is also included in the 71 RSSs. After the 71 RSSs are obtained, one stochastic response surface is constructed for each RSS using the second-order Hermite polynomial chaos expansion according to the procedure described in the "Multiple Stochastic Response Surfaces for RSSs" section. This results in 71 stochastic response surfaces. For example, the stochastic response surface for the CDSS in this example is given by

$$FS_{\mathrm{CDSS}}\left(\underline{\boldsymbol{\xi}}\right) = a_0\Gamma_0 + \sum_{i_1=1}^{15} a_{i_1}\Gamma_1\left(\xi_{i_1}\right) + \sum_{i_1=1}^{15}\sum_{i_2=1}^{i_1} a_{i_1,i_2}\Gamma_2\left(\xi_{i_1},\xi_{i_2}\right) \tag{7}$$

The values of coefficients $\mathbf{a} = \{a_0, a_{i_1}, a_{i_1,i_2}\}$ in Eq. (7) are given in Table 1. The 71 stochastic response surfaces can be verified by comparing the $FS_{\min}$ of slope stability obtained from the stochastic

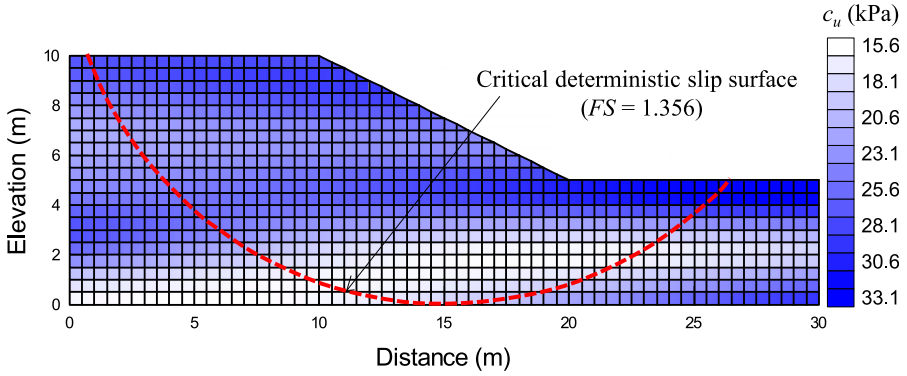

Fig. 2. Example of a cohesive slope

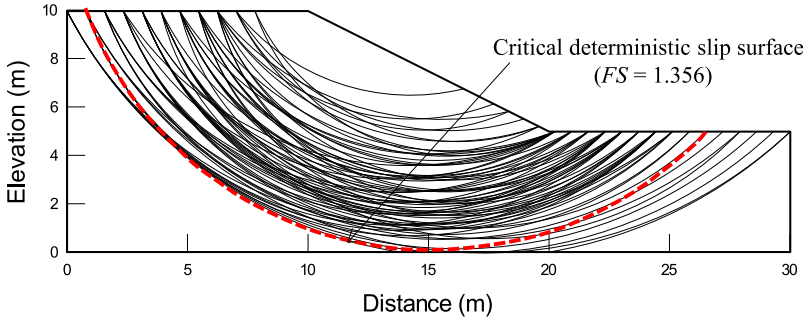

Fig. 3. The cohesive slope example's 71 RSSs ($\mathrm{COV}_{c_u} = 0.3$)

Table 1. Coefficients of the Stochastic Response Surface for the Critical Deterministic Slip Surface in Example I

Number	**a**	Value
0	a_0	1.3762
1	a_1	−0.1840
2	a_2	−0.1254
3	a_3	0.0812
4	a_4	−0.0267
5	a_5	0.0225
6	a_6	−0.0300
7	a_7	0.0117
8	a_8	−0.0014
9	a_9	0.0004
10	a_{10}	0.0010
11	a_{11}	−0.0008
12	a_{12}	−0.0010
13	a_{13}	0.0063
14	a_{14}	0.0227
15	a_{15}	−0.0022
16	$a_{1,1}$	0.0135
17	$a_{2,1}$	0.0173
18	$a_{2,2}$	0.0137
19	$a_{3,1}$	−0.0068
20	$a_{3,2}$	−0.0138
21	$a_{3,3}$	0.0100
22	$a_{4,1}$	0.0012
23	$a_{4,2}$	0.0049
24	$a_{4,3}$	−0.0087
25	$a_{4,4}$	0.0055
26	$a_{5,1}$	−0.0034
27	$a_{5,2}$	0.0029
28	$a_{5,3}$	−0.0005
29	$a_{5,4}$	−0.0009
30	$a_{5,5}$	0.0042
31	$a_{6,1}$	0.0038
32	$a_{6,2}$	−0.0020
33	$a_{6,3}$	−0.0011
34	$a_{6,4}$	−0.0002
35	$a_{6,5}$	0.0019
36	$a_{6,6}$	0.0028
37	$a_{7,1}$	0
38	$a_{7,2}$	−0.0003
39	$a_{7,3}$	0.0015
40	$a_{7,4}$	−0.0035
41	$a_{7,5}$	0.0001
42	$a_{7,6}$	0.0002
43	$a_{7,7}$	0.0027
44	$a_{8,1}$	−0.0005
45	$a_{8,2}$	−0.0017
46	$a_{8,3}$	−0.0011
47	$a_{8,4}$	−0.0019
48	$a_{8,5}$	0.0007
49	$a_{8,6}$	0.0003
50	$a_{8,7}$	0.0003
51	$a_{8,8}$	0.0019
52	$a_{9,1}$	0.0001
53	$a_{9,2}$	0.0010
54	$a_{9,3}$	−0.0018
55	$a_{9,4}$	−0.0009
56	$a_{9,5}$	−0.0011
57	$a_{9,6}$	−0.0006
58	$a_{9,7}$	−0.0004
59	$a_{9,8}$	0
60	$a_{9,9}$	0.0010
61	$a_{10,1}$	−0.0004
62	$a_{10,2}$	−0.0014
63	$a_{10,3}$	0.0010
64	$a_{10,4}$	−0.0003
65	$a_{10,5}$	0.0001
66	$a_{10,6}$	−0.0002
67	$a_{10,7}$	−0.0012
68	$a_{10,8}$	0.0004
69	$a_{10,9}$	0
70	$a_{10,10}$	0.0009
71	$a_{11,1}$	0.0003
72	$a_{11,2}$	0.0001
73	$a_{11,3}$	0.0003
74	$a_{11,4}$	−0.0006
75	$a_{11,5}$	0.0002
76	$a_{11,6}$	0.0005
77	$a_{11,7}$	−0.0001
78	$a_{11,8}$	−0.0005
79	$a_{11,9}$	0.0005
80	$a_{11,10}$	−0.0003
81	$a_{11,11}$	0.0004
82	$a_{12,1}$	0.0009
83	$a_{12,2}$	−0.0022
84	$a_{12,3}$	0.0018
85	$a_{12,4}$	−0.0008
86	$a_{12,5}$	−0.0004
87	$a_{12,6}$	0.0009
88	$a_{12,7}$	0.0002
89	$a_{12,8}$	0.0005
90	$a_{12,9}$	−0.0001
91	$a_{12,10}$	−0.0001
92	$a_{12,11}$	0.0001
93	$a_{12,12}$	0.0002
94	$a_{13,1}$	−0.0010
95	$a_{13,2}$	−0.0014
96	$a_{13,3}$	0.0015
97	$a_{13,4}$	−0.0011
98	$a_{13,5}$	0
99	$a_{13,6}$	−0.0001
100	$a_{13,7}$	0.0002
101	$a_{13,8}$	−0.0002
102	$a_{13,9}$	−0.0004
103	$a_{13,10}$	0.0008
104	$a_{13,11}$	0
105	$a_{13,12}$	0.0002
106	$a_{13,13}$	0.0005
107	$a_{14,1}$	−0.0023
108	$a_{14,2}$	−0.0018
109	$a_{14,3}$	0.0033
110	$a_{14,4}$	−0.0019
111	$a_{14,5}$	0.0008
112	$a_{14,6}$	−0.0009
113	$a_{14,7}$	0.0006
114	$a_{14,8}$	0
115	$a_{14,9}$	−0.0002
116	$a_{14,10}$	0.0004
117	$a_{14,11}$	0
118	$a_{14,12}$	0.0002

Table 1. (*Continued.*)

Number	a	Value
119	$a_{14,13}$	0.0002
120	$a_{14,14}$	0.0004
121	$a_{15,1}$	−0.0001
122	$a_{15,2}$	−0.0003
123	$a_{15,3}$	0
124	$a_{15,4}$	0.0002
125	$a_{15,5}$	0
126	$a_{15,6}$	−0.0004
127	$a_{15,7}$	−0.0003
128	$a_{15,8}$	0.0009
129	$a_{15,9}$	−0.0001
130	$a_{15,10}$	−0.0001
131	$a_{15,11}$	−0.0003
132	$a_{15,12}$	0.0001
133	$a_{15,13}$	0.0003
134	$a_{15,14}$	0.0001
135	$a_{15,15}$	0

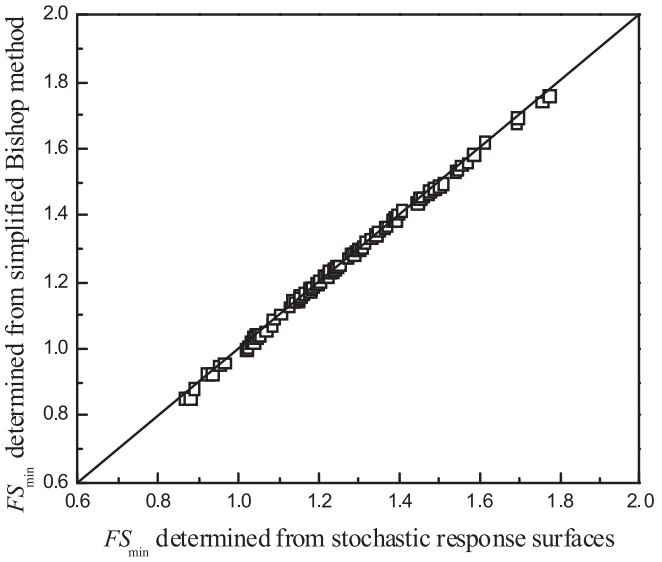

Fig. 4. Validation of stochastic response surfaces in the cohesive slope example

response surfaces and the original deterministic analysis (e.g., simplified Bishop method) of slope stability. Fig. 4 shows the $FS_{\min}$ values obtained from the 71 stochastic response surfaces using 100 sets of random samples versus those obtained from the simplified Bishop method. The $FS_{\min}$ values obtained from the two approaches agree well with each other. This indicates that the stochastic response surfaces are good enough to obtain $FS_{\min}$ in this example.

For the 71 stochastic response surfaces, a MCS run with $N_t = 500{,}000$ random samples is performed to calculate $P_{f,s}$, in which only the number (i.e., 15) of standard normal random variables contained in each stochastic response surface and the coefficients of the 71 stochastic response surfaces are used as inputs. Although a relatively large number (i.e., 500,000) of random samples are generated during the MCS, the computational costs used for the MCS are minimal and negligible, because it is performed using explicit functions (i.e., 71 stochastic response surfaces), by which $FS_{\min}$ can be solved instantaneously for each random sample.

System Reliability Analysis Results

Table 2 summarizes the reliability analysis results of this slope example obtained from this study and reported by Cho (2010). The system failure probability $P_{f,s}$ estimated from the proposed approach is 7.9×10^{-2}, which is in good agreement with that (i.e., 7.6×10^{-2}) obtained from the MCS using 100,000 random samples and the simplified Bishop method by Cho (2010). Such good agreement validates the proposed approach and indicates that the reduced series system comprised of 71 RSSs represents the slope reasonably well. Note that the $P_{f,s}$ in this example is on the order of magnitude of 10^{-2}, for which the 1,000 LHS samples used to construct the stochastic response surfaces are sufficient to calculate $P_{f,s}$. The value of $P_{f,s}$ estimated from the 1,000 LHS samples is 8.3×10^{-2} (Table 2) and agrees well with that obtained from the proposed approach. It does not seem necessary to construct the stochastic response surfaces and perform the MCS with stochastic response surfaces to calculate $P_{f,s}$ in this example. However, this is not true for the cases with relatively small values of $P_{f,s}$, e.g., $P_{f,s} < 0.001$. This is further discussed in the "Computational Efficiency at Small Probability Levels" section.

Computational Efficiency at Small Probability Levels

For example, as the COV_{c_u} decreases to 0.15 in this example, $P_{f,s}$ decreases significantly and is calculated as 2.8×10^{-4} using the proposed approach (Table 3). During the calculation, 1,000 random samples are again generated using LHS for the construction of stochastic response surfaces, and a MCS run with 500,000 random samples is performed to obtain $P_{f,s}$ based on the stochastic response surfaces. Note that there is no failure sample among the 1,000 random samples generated by LHS. In other words, 1,000 random samples are not sufficient to calculate $P_{f,s}$ when $\mathrm{COV}_{c_u} = 0.15$ in this example, because $P_{f,s}$ (i.e., 2.8×10^{-4}) is relatively small. To validate the value of $P_{f,s}$ obtained from the proposed approach, LHS is performed with 40,000 samples to recalculate $P_{f,s}$, where the simplified Bishop method is used to calculate $FS_{\min}$ for each random sample. The resulting $P_{f,s}$ is 3.8×10^{-4}, as shown in Table 3. The $P_{f,s}$ value (3.8×10^{-4}) obtained from the LHS with 40,000 samples compares favorably with that (e.g., 2.8×10^{-4}) estimated from the proposed approach.

Note that the computational efforts for the proposed approach contain those used for both the construction of stochastic response surfaces and the subsequent MCS based on stochastic response surfaces. As mentioned previously, 1,000 realizations of random field are generated in this example. Subsequently, 1,000 deterministic slope stability analyses are performed to estimate $FS_{\min}$ using the simplified Bishop method and to determine the RSSs, which are used to construct stochastic response surfaces. In this study, it takes approximately 38 s for each realization of the random field and the determination of its corresponding critical slip surface and $FS_{\min}$ on a desktop computer with 4-GB random-access memory (RAM) and one Intel Core i3 CPU clocked at 3.3 GHz. In addition, the total computational time for the MCS with 500,000 random samples using the stochastic response surfaces is approximately 70 s, which is equivalent to that used for approximately $70/38 \approx 2$ realizations of random field and the corresponding calculations of $FS_{\min}$ using the simplified Bishop method. Therefore, the total computational effort in the proposed approach is equivalent to that used for $1{,}000 + 2 = 1{,}002$ realizations of random field and 1,002 evaluations of $FS_{\min}$ using the simplified Bishop method. This effort is much less than that used for the direct implementation of LHS with 40,000 realizations of $\underline{c}_u$ and evaluations of $FS_{\min}$ using the simplified Bishop method. The proposed approach calculates the system failure probability $P_{f,s}$ efficiently at small probability levels.

Table 2. Reliability Analysis Results in Example I ($COV_{c_u} = 0.3$)

Method	Probability of failure $P(F)$	Source
RSSs + stochastic response surfaces + MCS	7.9×10^{-2}	This study
Limit-equilibrium method + LHS (1,000)	8.3×10^{-2}	This study
Limit-equilibrium method + MCS (100,000)	7.6×10^{-2}	Cho (2010)
CDSS + stochastic response surface + MCS	4.0×10^{-2}	This study
CDSS + limit-equilibrium method + MCS (100,000)	3.16×10^{-2}	Cho (2010)

Table 3. Reliability Analysis Results in Example I ($COV_{c_u} = 0.15$)

Method	Probability of failure $P(F)$	Source
RSSs + stochastic response surfaces + MCS	2.8×10^{-4}	This study
Limit-equilibrium method + LHS (1,000)	0	This study
Limit-equilibrium method + LHS (40,000)	3.8×10^{-4}	This study

In addition, based on the stochastic response surface of the CDSS in the nominal case, the failure probability $P_{f,\mathrm{CDSS}}$ of the CDSS is also estimated using a MCS in this study, and it is equal to 4.0×10^{-2}, which compares favorably with that (e.g., 3.16×10^{-2}) reported by Cho (2010). This further validates the proposed approach. It is also worthwhile to note that $P_{f,\mathrm{CDSS}}$ (i.e., 4.0×10^{-2}) is less than $P_{f,s}$ (i.e., 7.9×10^{-2}). The failure probability of slope stability is underestimated when only the CDSS is considered in the slope reliability analysis for the cohesive slope example.

Effects of Spatial Variability on System Reliability of Slope Stability

With the aid of the improved computational efficiency offered by the proposed approach, the effects of horizontal and vertical spatial variability on the system reliability of slope stability are explored through a series of sensitivity studies in this example. For the consideration of different spatial correlations, the sensitivity studies are performed with $\theta_{\ln,h}$ varying from 10 to 40 m and $\theta_{\ln,v}$ varying from 0.5 to 3.0 m. For each combination of $\theta_{\ln,h}$ and $\theta_{\ln,v}$, the proposed approach is applied to determine the RSSs and their corresponding stochastic response surfaces and then to estimate the system failure probability $P_{f,s}$ and failure probability $P_{f,\mathrm{CDSS}}$ of CDSS using the MCS and stochastic response surfaces.

Fig. 5(a) shows the variation of $P_{f,s}$ estimated from the proposed approach as a function of $\theta_{\ln,h}$ by a line with squares. The results are obtained for $\theta_{\ln,h}$ varying from 10 to 40 m and $\theta_{\ln,v} = 2.0$ m. For a given $\theta_{\ln,v} = 2.0$ m, $P_{f,s}$ increases from 5.9 to 8.9% as $\theta_{\ln,h}$ increases from 10 to 40 m. Overestimation of the horizontal spatial correlation (i.e., underestimation of the horizontal spatial variability) leads to a slight overestimation of $P_{f,s}$ at small probability levels. In addition, Fig. 5(b) shows the variation of $P_{f,s}$ estimated from the proposed approach as a function of $\theta_{\ln,v}$ by a line with squares. The results are obtained for $\theta_{\ln,h} = 20$ m and $\theta_{\ln,v}$ varying from 0.5 to 3.0 m. For a given $\theta_{\ln,h} = 20$ m, $P_{f,s}$ increases from 0.5 to 10.5% as $\theta_{\ln,v}$ increases from 0.5 to 3.0 m. Overestimation of the vertical spatial correlation (i.e., underestimation of the vertical spatial variability) leads to a significant overestimation of $P_{f,s}$ at small probability levels. From a physical point of view, overestimation of the vertical spatial correlation results in relatively slow variation in the simulated values of soil strength parameters along the depth. If a weak point is generated during the random field simulation, the points above or below it have a greater chance to be weak. In other words, the probability of forming a weak zone during random field simulation increases at small probability levels as the vertical spatial correlation is overestimated. This subsequently leads to an overestimation of $P_{f,s}$. In addition, it is noted that the vertical spatial variability has a much more significant effect on $P_{f,s}$ than the horizontal spatial variability. Such observations on the effects of spatial variability are consistent with those reported in the literature (Cho 2007; Ji et al. 2012).

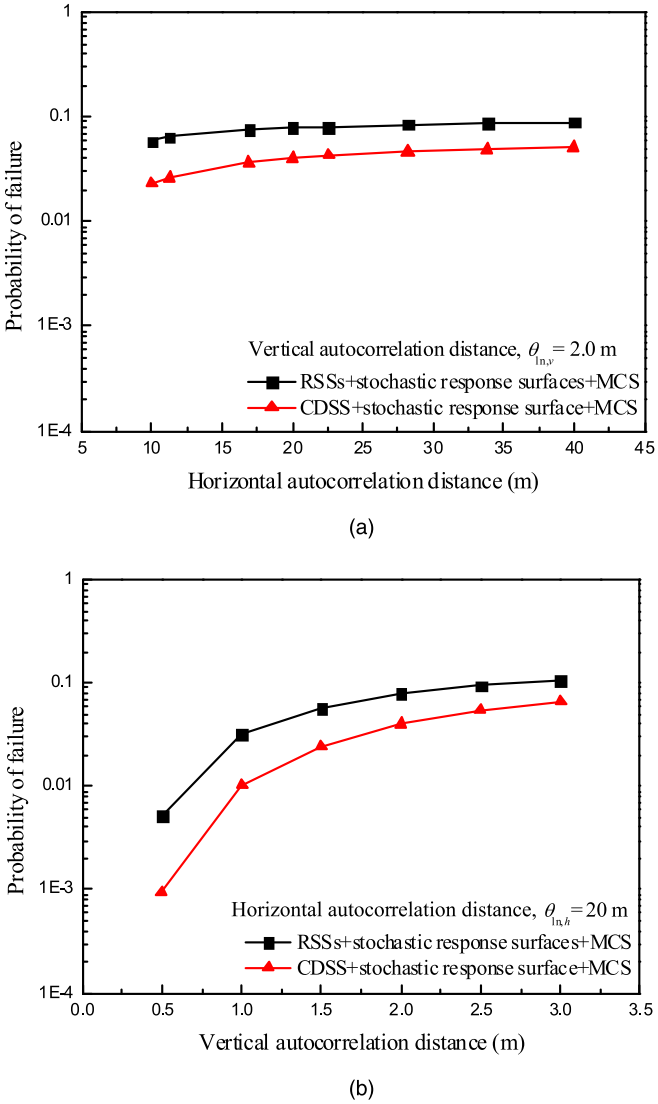

Fig. 5. Effects of spatial variability on the system failure probability of slope stability

From a system analysis point of view, the estimated $P_{f,s}$ relies on two factors: the number N_r of components (i.e., RSSs or dominating failure modes) in the reduced series system and the failure probability of each component (i.e., each RSS). Generally speaking, the $P_{f,s}$ increases as the number of RSSs and the failure probability of

each RSS increase. The failure probability of a given slip surface usually increases with the increase of $\theta_{\ln,v}$ at small probability levels, because the variance of sliding resistance along the slip surface increases as $\theta_{\ln,v}$ increases (Li and Lumb 1987; Cho 2007; Wang et al. 2011). For example, Figs. 5(a and b) show the respective variations of the failure probability $P_{f,\mathrm{CDSS}}$ of CDSS in the normal case as a function of horizontal and vertical autocorrelation distances by lines with triangles. As both horizontal and vertical autocorrelation distances increase, $P_{f,\mathrm{CDSS}}$ increases. For more details and theoretical explanations on the effects of vertical spatial variability on failure probability for a given slip surface, the reader is referred to Wang et al. (2011). On the other hand, Figs. 6(a and b) show the variations of N_r as a function of horizontal and vertical autocorrelation distances, respectively. As $\theta_{\ln,h}$ increases from 10 to 40 m, N_r decreases from 115 to 40 [Fig. 6(a)], which tends to make $P_{f,s}$ decrease. However, as shown in Fig. 5(a), $P_{f,s}$ increases as $\theta_{\ln,h}$ increases. This indicates that the effects of the decrease in N_r (i.e., the decrease in the number of components of the series system) on $P_{f,s}$ are dominated by those of the increase in the failure probability of each RSS on $P_{f,s}$ as $\theta_{\ln,h}$ increases. In addition, as $\theta_{\ln,v}$ increases from 0.5 to 3.0 m, N_r is more or less approximately 65, as shown in Fig. 6(b). Compared with the variation of N_r with the change in horizontal spatial correlation [Fig. 6(a)], the variation of N_r with the change in vertical spatial correlation is relatively minor [Fig. 6(b)]. However, as shown in Fig. 5(b), $P_{f,s}$ increases significantly as $\theta_{\ln,v}$ increases from 0.5 to 3.0 m. Such a significant increase in $P_{f,s}$ is mainly attributed to the increase of failure probability of each RSS at small probability levels as $\theta_{\ln,v}$ increases. Therefore, the spatial variability in both horizontal and vertical directions affects the system failure probability and the failure probability of a given slip surface in a consistent manner. The effects of spatial variability on the failure probability of each individual slip surface dominate those on the number of RSSs and are subsequently reflected in the slope system failure probability.

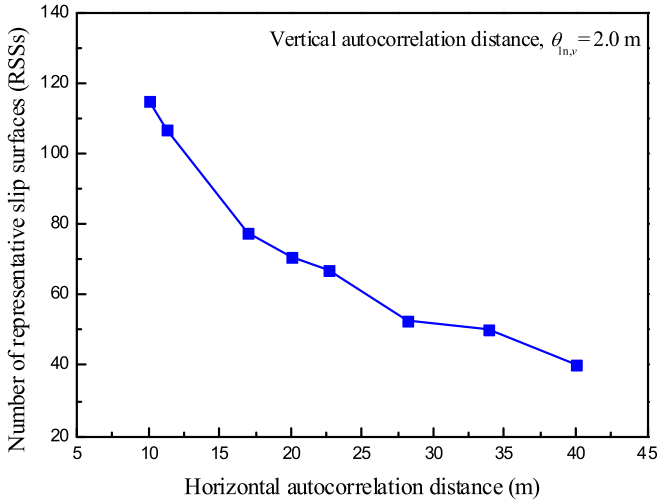

(a)

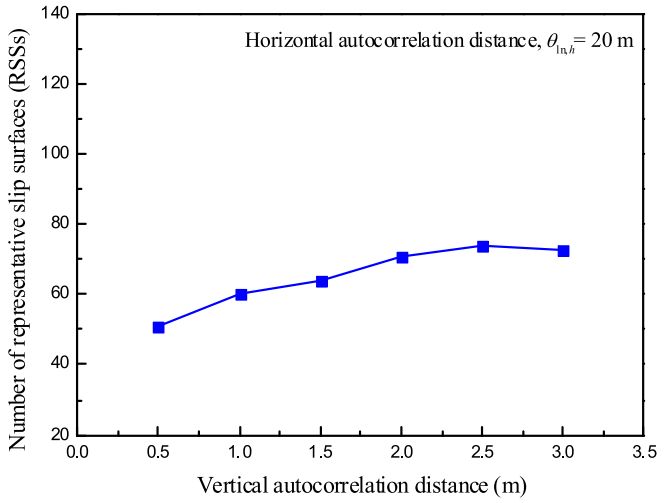

(b)

Fig. 6. Effects of spatial variability on the number of RSSs

Recommendations for Determining the Values of Autocorrelation Distances in Slope Design

To incorporate the inherent spatial variability into slope design in practice, there exists a need to determine $\theta_{\ln,h}$ and $\theta_{\ln,v}$ for a specific site. When the values of $\theta_{\ln,h}$ and $\theta_{\ln,v}$ are available for a specific site, using their site-specific values in slope design is recommended. However, this is rarely the case, because site observation data obtained from geotechnical site characterization are generally too sparse to generate statistically meaningful estimates of $\theta_{\ln,h}$ and $\theta_{\ln,v}$ for a specific site. Although site-specific values of these parameters are rarely available, some possible values of them were reported in the geotechnical literature according to global data. Based on a literature review, the recommended ranges of $\theta_{\ln,h}$ and $\theta_{\ln,v}$ are obtained, and they are [10 m, 40 m] for $\theta_{\ln,h}$ and [0.5 m, 3.0 m] for $\theta_{\ln,v}$ (Phoon and Kulhawy 1999; El-Ramly et al. 2003; Ji et al. 2012; Salgado and Kim 2014). In case of no available information on $\theta_{\ln,h}$ and $\theta_{\ln,v}$ obtained from a specific site in practice, the recommendation is to use the values within their respective possible ranges (e.g., [10 m, 40 m] and [0.5 m, 3.0 m] for $\theta_{\ln,h}$ and $\theta_{\ln,v}$, respectively) reported in the literature to perform systematic sensitivity studies to explore their effects on slope system reliability. For example, a sensitivity study is performed in the "Effects of Spatial Variability on System Reliability of Slope Stability" section to explore the effects of $\theta_{\ln,h}$ and $\theta_{\ln,v}$ on slope system reliability in this example. The results of the sensitivity study may further assist in choosing the values of $\theta_{\ln,h}$ and $\theta_{\ln,v}$ in slope design practice. As shown in Fig. 5, $P_{f,s}$ increases as $\theta_{\ln,h}$ and $\theta_{\ln,v}$ increase. In this case, the upper bounds (e.g., 40 and 3.0 m, respectively) of their possible ranges reported in the literature are recommended to be used in slope design practice if no site-specific information on $\theta_{\ln,h}$ and $\theta_{\ln,v}$ is available. This, of course, subsequently leads to relatively conservative designs in this example.

Illustrative Example II: *c*-ϕ Slope

For further illustration, this section applies the proposed approach to analyze a *c*-ϕ slope example and to explore effects of cross-correlation between c and ϕ on the system reliability of slope stability. Fig. 7 shows a *c*-ϕ slope with a height of 10 m and a slope angle of 45°, which was analyzed by Cho (2010) using MCS and the simplified Bishop method. The *c*-ϕ soil layer extends to 15 m below the top of the slope and has a total unit weight of 20 kN/m^3. In the soil layer, the inherent spatial variability of the cohesion and friction angle is characterized by two cross-correlated 2D lognormal stationary random fields $\underline{c}$ and $\underline{\phi}$. The random field $\underline{c}$ has a mean value of 10 kPa (i.e., $\mu_c = 10$ kPa) and COV of 0.3 (i.e., $\mathrm{COV}_c = 0.3$), and the random field $\underline{\phi}$ has a mean value of 30° (i.e., $\mu_\phi = 30°$) and COV of 0.2 (i.e., $\mathrm{COV}_\phi = 0.2$). Then, $\theta_{\ln,h}$ and $\theta_{\ln,v}$ in both $\underline{c}$ and $\underline{\phi}$ are

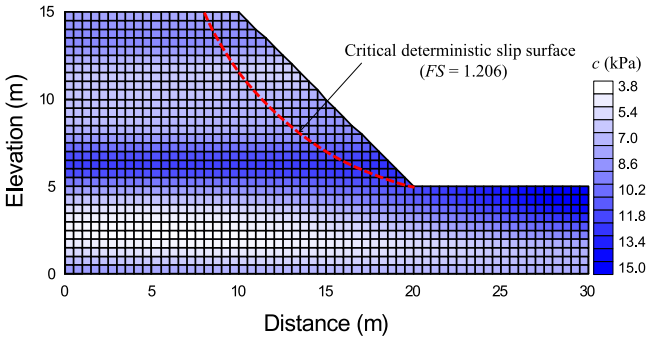

Fig. 7. Example of a c-ϕ slope

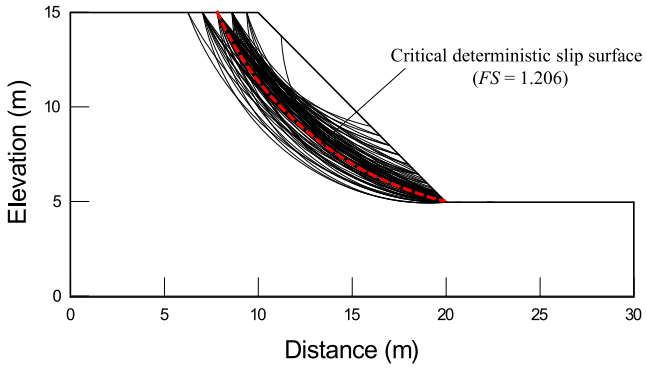

Fig. 8. The c-ϕ slope example's 79 RSSs

taken as 20 and 2 m, respectively. In addition, the cross-correlation coefficient between c and ϕ is taken as -0.7. The statistics of c and ϕ used in this study are consistent with those adopted by Cho (2010). For the realization of random fields, both $\underline{c}$ and $\underline{\phi}$ are discretized into 1,210 elements with a side length of 0.5 m (Fig. 7), and their random samples are then generated using Eqs. (3) and (4) at the centroid of each element, where M is taken to be 20 for each random field in this example. As a reference, the nominal value of $FS_{\min}$ that corresponds to the case of all the c and ϕ equal to their respective mean values (i.e., 10 kPa and 30°) is calculated using the simplified Bishop method, and it is equal to 1.206, which is almost identical to the value (i.e., 1.204) reported by Cho (2010). In addition, the critical slip surface in the nominal case is also located and shown in Fig. 7. It is referred to as the CDSS in this example.

For the identification of RSSs and the construction of their respective stochastic response surfaces, 1,000 realizations (i.e., $N_p = 1{,}000$) of $\underline{c}$ and $\underline{\phi}$ are simulated by LHS using Eqs. (3) and (4), and their corresponding critical slip surfaces are determined using the simplified Bishop method and taken as RSSs in this example, resulting in a total of 79 RSSs, as shown in Fig. 8. Note that the CDSS in the nominal case (see the dashed line in Fig. 8) is also included in the 79 RSSs. After the 79 RSSs are obtained, one stochastic response surface is constructed accordingly for each RSS using the second-order Hermite polynomial chaos expansion, resulting in 79 stochastic response surfaces. Based on these stochastic response surfaces, a MCS run with 500,000 random samples is performed to calculate $P_{f,s}$. Similar to Example I, the computational costs used for the MCS are minimal and negligible, although a large number (i.e., 500,000) of random samples are generated during the MCS.

System Reliability Analysis Results

Table 4 summarizes the reliability analysis results of this slope example obtained from this study and reported by Cho (2010). The system failure probability $P_{f,s}$ estimated from the proposed approach is 4.9×10^{-3}, which compares favorably with the result (i.e., 3.9×10^{-3}) obtained from the MCS using 50,000 random samples and the simplified Bishop method by Cho (2010). The slight difference between the results might be attributed to the fact that different autocorrelation functions are used in this study and Cho (2010). A squared exponential autocorrelation function [Eq. (1)] is used in this study. However, a single exponential autocorrelation function is used by Cho (2010). Although the single exponential autocorrelation function is commonly used in the literature, it usually necessitates more terms (i.e., a larger value of M) to ensure the desired accuracy of the truncated representation of the random field using a K-L expansion compared with the squared exponential autocorrelation function. As M decreases, the computational efficiency of

Table 4. Reliability Analysis Results in Example II

Method	Probability of failure $P(F)$	Source
RSSs + Stochastic response surfaces + MCS	4.9×10^{-3}	This study
Limit-equilibrium method + LHS (1,000)	3.0×10^{-3}	This study
Limit-equilibrium method + LHS (10,000)	4.4×10^{-3}	This study
Limit-equilibrium method + MCS (50,000)	3.9×10^{-3}	Cho (2010)

random field generation using the K-L expansion improves. Hence, the squared exponential autocorrelation function is adopted in this study, rather than the single exponential autocorrelation function. In addition, previous studies have demonstrated that the forms of autocorrelation functions have no significant effects on the reliability of slope stability (Li and Lumb 1987), particularly when the scale of fluctuation is relatively small compared with the dimension of the slip surface. This is consistent with the observations obtained from this study.

Note that $P_{f,s}$ in this example is on the order of magnitude of 10^{-3}. It is also interesting to take a look at $P_{f,s}$ obtained from the 1,000 LHS samples used to construct the stochastic response surfaces at this order of magnitude. It is found that $P_{f,s}$ obtained from the 1,000 LHS samples is 3.0×10^{-3} (Table 4). This indicates that there are only three failure samples among the 1,000 LHS samples, which are too few to generate a meaningful estimate of $P_{f,s}$. The 1,000 LHS samples are not sufficient to calculate $P_{f,s}$ at an order of magnitude of 10^{-3}. To further validate the proposed approach, LHS with 10,000 random samples is also performed to calculate the system failure probability, where $FS_{\min}$ is directly evaluated using the simplified Bishop method with a consideration of numerous potential slip surfaces and a squared exponential autocorrelation function given by Eq. (1) is used to simulate random fields. As shown in Table 4, the value of $P_{f,s}$ obtained from the LHS with 10,000 samples and the simplified Bishop method is 4.4×10^{-3}, which agrees well with the result (i.e., 4.9×10^{-3}) obtained from the proposed approach. The value of $P_{f,s}$ is efficiently calculated using the proposed approach with reasonable accuracy.

Effects of Cross-Correlation on System Reliability of Slope Stability

To explore the effects of cross-correlation between c and ϕ on the system reliability of slope stability, a sensitivity study is performed with $\rho_{c\text{-}\phi}$ varying from -0.7 to 0. For each value of $\rho_{c\text{-}\phi}$, the proposed approach is applied to determine the RSSs and their corresponding stochastic response surfaces and to evaluate $P_{f,s}$ and

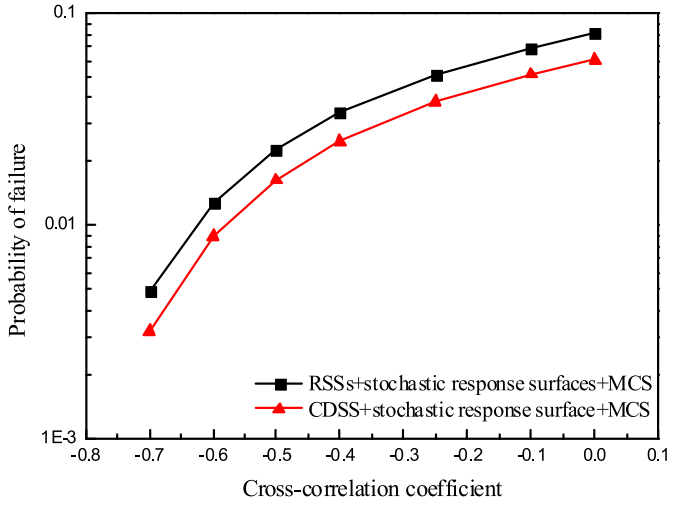

Fig. 9. Effects of cross-correlation on the system failure probability of slope stability

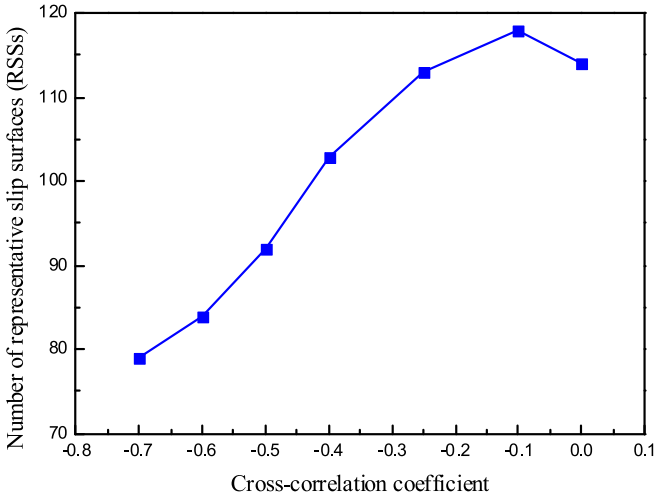

Fig. 10. Effects of cross-correlation on the number of RSSs

$P_{f,\mathrm{CDSS}}$. Fig. 9(a) shows the variation of $P_{f,s}$ as a function $\rho_{c\text{-}\phi}$ by a line with squares. As $\rho_{c\text{-}\phi}$ varies from -0.7 to 0, the estimated $P_{f,s}$ increases from 0.49 to 8%. The cross-correlation between c and ϕ significantly affects $P_{f,s}$. Note that the cross-correlation between c and ϕ is assumed to be negative (i.e., $\rho_{c\text{-}\phi} < 0$) in this study. Then, the increase of c often corresponds to the decrease of ϕ. As the negative correlation between c and ϕ becomes stronger (i.e., $\rho_{c\text{-}\phi}$ varies from 0 to -0.7), this trend becomes stronger, and the variance of the soil total shear strength (including both c and ϕ) decreases (Fenton and Griffiths 2003; Cho 2010). This may subsequently lead to a significant decrease in the failure probability of slope stability at small probability levels. Hence, ignoring the negative cross-correlation between c and ϕ (i.e., $\rho_{c\text{-}\phi} = 0$) leads to an overestimation of $P_{f,s}$ and conservative designs at small probability levels.

Similar to the effects of spatial correlation, the effects of cross-correlation on $P_{f,s}$ can also be revisited from a system analysis point of view and are divided into two aspects: the effects on the number N_r of RSSs and on the failure probability of each RSS. Based on previous studies (Cho 2010; Wang et al. 2011; Li et al. 2011a, b), the failure probability of a given slip surface generally increases at small probability levels as the negative cross-correlation becomes weaker (i.e., the negative value of $\rho_{c\text{-}\phi}$ increases). For example, Fig. 9 also shows the variation of the failure probability $P_{f,\mathrm{CDSS}}$ of the CDSS as a function of the cross-correlation coefficient by a line with triangles. As the negative cross-correlation becomes weaker, $P_{f,\mathrm{CDSS}}$ increases. The effects of cross-correlation on the failure probability of a given slip surface are consistent with those on $P_{f,s}$. In addition, Fig. 10 shows that, as $\rho_{c\text{-}\phi}$ varies from -0.7 to 0, N_r generally increases from approximately 80 to approximately 115, which also tends to make $P_{f,s}$ increase. The effects of cross-correlation on the number N_r of RSSs and the failure probability of each RSS are consistent for the c-ϕ slope example, and they are combined together and reflected in the system reliability of slope stability as the cross-correlation varies.

Recommendations for Determining the Value of the Cross-Correlation Coefficient in Slope Design

It is also worthwhile to point out that the determination of $\rho_{c\text{-}\phi}$ for a specific site is not a trivial task in practice, because geotechnical site characterization usually provides a limited amount of c and ϕ data for the specific site. In case of no prevailing knowledge about $\rho_{c\text{-}\phi}$ for the specific site, the recommended values of $\rho_{c\text{-}\phi}$ can be obtained from the literature and the results of a sensitivity study. Similar to $\theta_{\ln,h}$ and $\theta_{\ln,v}$, the recommended range of $\rho_{c\text{-}\phi}$ is obtained from the literature, e.g., $[-0.7, 0]$ is used in this study (Lumb 1970; Yucemen et al. 1973; Tang et al. 2012). Then, using the values of $\rho_{c\text{-}\phi}$ within the recommended range, a sensitivity study can be performed to explore the effects of $\rho_{c\text{-}\phi}$ on the slope system reliability. Based on the results of the sensitivity study (Fig. 9), some recommended values of $\rho_{c\text{-}\phi}$ are obtained. For example, Fig. 9 shows that $P_{f,s}$ increases as $\rho_{c\text{-}\phi}$ increases. When no prevailing knowledge on $\rho_{c\text{-}\phi}$ is available from the specific site, the recommendation is to take $\rho_{c\text{-}\phi}$ to be zero, i.e., ignore the negative cross-correlation. This subsequently leads to an overestimation of $P_{f,s}$ and relatively conservative designs.

Discussion

The proposed approach facilitates the slope system reliability analysis using RSSs and multiple stochastic response surfaces. They are affected by the number (i.e., N_p) of realizations of random fields used to determine the unknown coefficients in the stochastic response surfaces, random field element mesh, and deterministic slope stability analysis method. The effects of these three factors on RSSs and the construction of stochastic response surfaces are discussed in this section.

In the proposed approach, RSSs are simultaneously identified from potential slip surfaces during the construction of stochastic response surfaces. The number (i.e., N_p) of random field realizations used to construct stochastic response surfaces affects the identification of RSSs. The determination of a reasonable N_p is pivotal to the identification of RSSs. In general, N_p shall be at least greater than the number [i.e., $(N + n_{\mathrm{HPCE}})!/(N! \times n_{\mathrm{HPCE}}!)$ in this study] of unknown coefficients in the stochastic response surfaces. For example, $N = 15$ and $n_{\mathrm{HPCE}} = 2$ are adopted for the case with $\mathrm{COV}_{c_u} = 0.3$ in Example I, which leads to $(15 + 2)!/(15! \times 2!) = 136$ unknown coefficients. In the example, N_p shall be greater than 136, and hence, $N_p = 1{,}000$ is adopted. As N_p increases, the number of RSSs tends to increase, because it is possible for slope failure to occur along more potential slip surfaces. Because each RSS corresponds to one stochastic response surface in the proposed approach, the number of

stochastic response surfaces used to estimate $P_{f,s}$ increases. This subsequently leads to a more accurate estimate of $P_{f,s}$, whereas the computational efficiency deceases as N_p increases. Then, the determination of N_p becomes a trade-off between the computational accuracy and efficiency.

Note that random fields are simulated at an element level in this study, by which the values of geotechnical parameters are simulated at the centroid of random field elements and are then assigned to these elements for slope stability analysis. As the random field element mesh becomes finer (e.g., the element size becomes smaller), the spatial variability of soil parameters is simulated in a more accurate and realistic way in the sense that the soil parameters vary from one point to another in reality. This might subsequently lead to more accurate estimates of the location of the critical slip surface and its *FS* value for each realization of random fields. Because RSSs are a collection of critical slip surfaces obtained during the construction of stochastic response surfaces, the RSSs are also affected by the random field element mesh. Using a finer random field element mesh may give more accurate predictions of locations of RSSs and their respective *FS* values. This subsequently affects the accuracy of stochastic response surfaces and $P_{f,s}$ as well.

In addition, it is also worthwhile to point out that the selected RSSs and their *FS* values also rely on the deterministic slope stability analysis method. In this study, the limit-equilibrium method with circular failure mechanism (i.e., simplified Bishop method) is applied to identify the RSSs and construct stochastic response surfaces. Therefore, all the RSSs are circular slip surfaces in this study. However, it should be noted that, when a deterministic slope stability analysis method that allows compound slip surfaces is applied, the compound failure mechanism might be included in the selected RSSs. Moreover, for a given RSS, the stochastic response surfaces calibrated from different deterministic slope stability analysis methods are different to some degree and may indicate different functional relationships between the system response concerned and input uncertain parameters.

Summary and Conclusions

This paper developed an efficient system reliability analysis approach based on MCS and limit-equilibrium analysis of slope stability to efficiently evaluate the system failure probability $P_{f,s}$ of slope stability in spatially variable soils. The proposed approach facilitates the slope system reliability analysis using RSSs and multiple stochastic response surfaces. Based on the RSSs and their corresponding stochastic response surfaces, $P_{f,s}$ is evaluated using MCS with negligible computation costs. The proposed MCS-based system reliability analysis approach was illustrated through a cohesive slope example and a c-ϕ slope example. The results showed that the approach estimates $P_{f,s}$ properly considering the spatial variability of the soil properties and improves the computational efficiency significantly at small probability levels. With the aid of the improved computational efficiency offered by the proposed approach, a series of sensitivity studies were carried out to explore the effects of spatial variability in both the horizontal and vertical directions and cross-correlation between uncertain soil parameters. The results showed that both the spatial variability and cross-correlation significantly affect the system reliability of slope stability in spatially variable soils. The proposed approach allows insights into the effects of spatial variability and cross-correlation on $P_{f,s}$ from a system analysis point of view. Finally, the factors that affect the accuracy of $P_{f,s}$ estimated from the proposed approach were also discussed.

Acknowledgments

This work was supported by the National Science Fund for Distinguished Young Scholars (Project No. 51225903), the National Basic Research Program of China (973 Program) (Project No. 2011CB013506), and the National Natural Science Foundation of China (Project No. 51329901).

Notation

The following symbols are used in this paper:

$\mathrm{COV}_H = \sigma_H/\mu_H$ = coefficient of variation of H;
$FS_{\min}$ = minimum factor of safety;
H = uncertain soil property of interest (i.e., c_u, c, or ϕ);
$\underline{H}(x,y)$ = 2D lognormal stationary random field;
N_p = number of random samples used to construct stochastic response surfaces;
N_r = number of RSSs;
N_s = number of potential slip surfaces;
N_t = total number of random samples generated during MCS;
$\theta_{\ln,h}$ = horizontal autocorrelation distance;
$\theta_{\ln,v}$ = vertical autocorrelation distance;
μ_H = mean of H;
$\mu_{N,H}$ = mean of $\ln(H)$;
$\xi_j(\theta), j = 1,2,\ldots,M$ = set of independent standard normal random variables;
$\rho_{c\text{-}\phi}$ = cross-correlation coefficient between c and ϕ at the same location;
$\rho_{c\text{-}\phi,N}$ = cross-correlation coefficient between $\ln(c)$ and $\ln(\phi)$ at the same location;
σ_H = SD of H;
$\sigma_{N,H}$ = SD of $\ln(H)$; and
$\chi_j(\theta), j = 1,2,\ldots,M$ = set of spatially correlated standard normal random variables.

References

Al-Bittar, T., and Soubra, A. H. (2013). "Bearing capacity of strip footings on spatially random soils using sparse polynomial chaos expansion." *Int. J. Numer. Anal. Methods Geomech.*, 37(13), 2039–2060.

Ching, J., and Phoon, K.-K. (2013). "Probability distribution for mobilised shear strengths of spatially variable soils under uniform stress states." *Georisk*, 7(3), 209–224.

Ching, J., Phoon, K.-K., and Hu, Y.-G. (2009). "Efficient evaluation of reliability for slopes with circular slip surfaces using importance sampling." *J. Geotech. Geoenviron. Eng.*, 10.1061/(ASCE)GT.1943-5606.0000035, 768–777.

Cho, S. E. (2007). "Effects of spatial variability of soil properties on slope stability." *Eng. Geol.*, 92(3–4), 97–109.

Cho, S. E. (2010). "Probabilistic assessment of slope stability that considers the spatial variability of soil properties." *J. Geotech. Geoenviron. Eng.*, 10.1061/(ASCE)GT.1943-5606.0000309, 975–984.

Cho, S. E. (2013). "First-order reliability analysis of slope considering multiple failure modes." *Eng. Geol.*, 154(Feb), 98–105.

Choi, S. K., Canfield, R. A., and Grandhi, R. V. (2006). "Estimation of structural reliability for Gaussian random fields." *Struct. Infrastruct. Eng.*, 2(3–4), 161–173.

Chowdhury, R. N., and Xu, D. W. (1995). "Geotechnical system reliability of slopes." *Reliab. Eng. Syst. Saf.*, 47(3), 141–151.

Christian, J. T., Ladd, C. C., and Baecher, G. B. (1994). "Reliability applied to slope stability analysis." *J. Geotech. Engrg.*, 10.1061/(ASCE)0733-9410(1994)120:12(2180), 2180–2207.

Cornell, C. A. (1967). "Bounds on the reliability of structural systems." *J. Struct. Div.*, 93(1), 171–200.
Ditlevsen, O. (1979). "Narrow reliability bounds for structural systems." *J. Struct. Mech.*, 7(4), 453–472.
Duncan, J. M., and Wright, S. G. (2005). *Soil strength and slope stability*, Wiley, Upper Saddle River, NJ.
El-Ramly, H., Morgenstern, N. R., and Cruden, D. M. (2002). "Probabilistic slope stability analysis for practice." *Can. Geotech. J.*, 39(3), 665–683.
El-Ramly, H., Morgenstern, N. R., and Cruden, D. M. (2003). "Probabilistic stability analysis of a tailings dyke on presheared clayshale." *Can. Geotech. J.*, 40(1), 192–208.
Fenton, G. A., and Griffiths, D. V. (2003). "Bearing-capacity prediction of spatially random $c\varphi$ soils." *Can. Geotech. J.*, 40(1), 54–65.
Fenton, G. A., and Griffiths, D. V. (2008). *Risk assessment in geotechnical engineering*, Wiley, New York.
Ghanem, R. G., and Spanos, P. D. (2003). *Stochastic finite element: A spectral approach*, Dover, Mineola, NY.
Griffiths, D. V., and Fenton, G. A. (2004). "Probabilistic slope stability analysis by finite elements." *J. Geotech. Geoenviron. Eng.*, 10.1061/(ASCE)1090-0241(2004)130:5(507), 507–518.
Griffiths, D. V., Fenton, G. A., and Manoharan, N. (2002). "Bearing capacity of rough rigid strip footing on cohesive soil: Probabilistic study." *J. Geotech. Geoenviron. Eng.*, 10.1061/(ASCE)1090-0241(2002)128:9(743), 743–755.
Huang, J. S., Griffiths, D. V., and Fenton, G. A. (2010). "System reliability of slopes by RFEM." *Soils Found.*, 50(3), 343–353.
Huang, S. P., Liang, B., and Phoon, K. K. (2009). "Geotechnical probabilistic analysis by collocation-based stochastic response surface method—An EXCEL add-in implementation." *Georisk*, 3(2), 75–86.
Ji, J., Liao, H. J., and Low, B. K. (2012). "Modeling 2-D spatial variation in slope reliability analysis using interpolated autocorrelations." *Comput. Geotech.*, 40(Mar), 135–146.
Ji, J., and Low, B. K. (2012). "Stratified response surfaces for system probabilistic evaluation of slopes." *J. Geotech. Geoenviron. Eng.*, 10.1061/(ASCE)GT.1943-5606.0000711, 1398–1406.
Jiang, S. H., Li, D. Q., Zhang, L. M., and Zhou, C. B. (2014a). "Slope reliability analysis considering spatially variable shear strength parameters using a non-intrusive stochastic finite element method." *Eng. Geol.*, 168(Jan), 120–128.
Jiang, S. H., Li, D. Q., Zhou, C. B., and Zhang, L. M. (2014b). "Capabilities of stochastic response surface method and response surface method in reliability analysis." *Struct. Eng. Mech.*, 49(1), 111–128.
Laloy, E., Rogiers, B., Vrugt, J. A., Mallants, D., and Jacques, D. (2013). "Efficient posterior exploration of a high-dimensional groundwater model from two-stage Markov chain Monte Carlo simulation and polynomial chaos expansion." *Water Resour. Res.*, 49(5), 2664–2682.
Li, D., Chen, Y., Lu, W., and Zhou, C. (2011a). "Stochastic response surface method for reliability analysis of rock slopes involving correlated non-normal variables." *Comput. Geotech.*, 38(1), 58–68.
Li, D., Zhou, C., Lu, W., and Jiang, Q. (2009). "A system reliability approach for evaluating stability of rock wedges with correlated failure modes." *Comput. Geotech.*, 36(8), 1298–1307.
Li, D.-Q., Jiang, S.-H., Chen, Y.-F., and Zhou, C.-B. (2011b). "System reliability analysis of rock slope stability involving correlated failure modes." *KSCE J. Civ. Eng.*, 15(8), 1349–1359.
Li, D.-Q., Qi, X.-H., Phoon, K.-K., Zhang, L.-M., and Zhou, C.-B. (2014). "Effect of spatially variable shear strength parameters with linearly increasing mean trend on reliability of infinite slopes." *Struct. Saf.*, 49, 45–55.
Li, K. S., and Lumb, P. (1987). "Probabilistic design of slopes." *Can. Geotech. J.*, 24(4), 520–535.
Li, L., Wang, Y., Cao, Z., and Chu, X. (2013). "Risk de-aggregation and system reliability analysis of slope stability using representative slip surfaces." *Comput. Geotech.*, 53(Sep), 95–105.
Lloret-Cabot, M., Fenton, G. A., and Hicks, M. A. (2014). "On the estimation of scale of fluctuation in geostatistics." *Georisk*, 8(2), 129–140.
Low, B. K., Zhang, J., and Tang, W. H. (2011). "Efficient system reliability analysis illustrated for a retaining wall and a soil slope." *Comput. Geotech.*, 38(2), 196–204.
Lumb, P. (1970). "Safety factors and the probability distribution of soil strength." *Can. Geotech. J.*, 7(3), 225–242.
Marzouk, Y. M., and Najm, H. N. (2009). "Dimensionality reduction and polynomial chaos acceleration of Bayesian inference in inverse problems." *J. Comput. Phys.*, 228(6), 1862–1902.
Oka, Y., and Wu, T. H. (1990). "System reliability of slope stability." *J. Geotech. Engrg.*, 10.1061/(ASCE)0733-9410(1990)116:8(1185), 1185–1189.
Phoon, K. K., Huang, S. P., and Quek, S. T. (2002). "Implementation of Karhunen-Loève expansion for simulation using a wavelet-Galerkin scheme." *Probab. Eng. Mech.*, 17(3), 293–303.
Phoon, K.-K., and Kulhawy, F. H. (1999). "Characterization of geotechnical variability." *Can. Geotech. J.*, 36(4), 612–624.
Salgado, R., and Kim, D. (2014). "Reliability analysis of load and resistance factor design of slopes." *J. Geotech. Geoenviron. Eng.*, 10.1061/(ASCE)GT.1943-5606.0000978, 57–73.
SLOPE/W 2007 [Computer software]. Calgary, AB, Canada, GEO-SLOPE International.
Tabarroki, M., Ahmad, F., Banaki, R., Jha, S. K., and Ching, J. (2013). "Determining the factors of safety of spatially variable slopes modeled by random fields." *J. Geotech. Geoenviron. Eng.*, 10.1061/(ASCE)GT.1943-5606.0000955, 2082–2095.
Tang, X.-S., Li, D.-Q., Chen, Y.-F., Zhou, C.-B., and Zhang, L.-M. (2012). "Improved knowledge-based clustered partitioning approach and its application to slope reliability analysis." *Comput. Geotech.*, 45(Sep), 34–43.
Vanmarcke, E. H. (1977a). "Probabilistic modeling of soil profiles." *J. Geotech. Engrg. Div.*, 103(11), 1227–1246.
Vanmarcke, E. H. (1977b). "Reliability of earth slopes." *J. Geotech. Engrg. Div.*, 103(11), 1247–1265.
Wang, Y. (2013). "MCS-based probabilistic design of embedded sheet pile walls." *Georisk*, 7(3), 151–162.
Wang, Y., Cao, Z. J., and Au, S.-K. (2011). "Practical reliability analysis of slope stability by advanced Monte Carlo simulations in a spreadsheet." *Can. Geotech. J.*, 48(1), 162–172.
Yucemen, M. S., Tang, W. H., and Ang, H.-S. (1973). *A probability study of safety and design of earth slopes*, Univ. of Illinois, Urbana, IL.
Zhang, J., Huang, H. W., and Phoon, K. K. (2013). "Application of the kriging-based response surface method to the system reliability of soil slopes." *J. Geotech. Geoenviron. Eng.*, 10.1061/(ASCE)GT.1943-5606.0000801, 651–655.
Zhang, J., Zhang, L. M., and Tang, W. H. (2011). "New methods for system reliability analysis of soil slopes." *Can. Geotech. J.*, 48(7), 1138–1148.